Psychological Medicine

cambridge.org/psm

Structure-function coupling and hierarchy-specific antidepressant response in major depressive disorder

Xinyi Wang[1,2], Li Xue[1,2], Lingling Hua[3], Junneng Shao[1,2], Rui Yan[3], Zhijian Yao[3,4] and Qing Lu[1,2]

[1]School of Biological Sciences & Medical Engineering, Southeast University, Nanjing, China; [2]Child Development and Learning Science, Key Laboratory of Ministry of Education, Southeast University, Nanjing, China; [3]Department of Psychiatry, the Affiliated Brain Hospital of Nanjing Medical University, Nanjing, China and [4]Nanjing Brain Hospital, Clinical Teaching Hospital of Medical School, Nanjing University, Nanjing, China

Original Article

Cite this article: Wang X, Xue L, Hua L, Shao J, Yan R, Yao Z, Lu Q (2024). Structure-function coupling and hierarchy-specific antidepressant response in major depressive disorder. *Psychological Medicine* **54**, 2688–2697. https://doi.org/10.1017/S0033291724000801

Received: 21 September 2023
Revised: 9 February 2024
Accepted: 4 March 2024
First published online: 4 April 2024

Keywords:
antidepressant response; brain hierarchy; functional connectivity gradient; structure-function coupling

Corresponding author:
Qing Lu;
Email: luq@seu.edu.cn;
Zhijian Yao;
Email: zjyao@njmu.edu.cn

Abstract

Background. Extensive research has explored altered structural and functional networks in major depressive disorder (MDD). However, studies examining the relationships between structure and function yielded heterogeneous and inconclusive results. Recent work has suggested that the structure-function relationship is not uniform throughout the brain but varies across different levels of functional hierarchy. This study aims to investigate changes in structure-function couplings (SFC) and their relevance to antidepressant response in MDD from a functional hierarchical perspective.

Methods. We compared regional SFC between individuals with MDD ($n = 258$) and healthy controls (HC, $n = 99$) using resting-state functional magnetic resonance imaging and diffusion tensor imaging. We also compared antidepressant non-responders ($n = 55$) and responders ($n = 68$, defined by a reduction in depressive severity of >50%). To evaluate variations in altered and response-associated SFC across the functional hierarchy, we ranked significantly different regions by their principal gradient values and assessed patterns of increase or decrease along the gradient axis. The principal gradient value, calculated from 219 healthy individuals in the Human Connectome Project, represents a region's position along the principal gradient axis.

Results. Compared to HC, MDD patients exhibited increased SFC in unimodal regions (lower principal gradient) and decreased SFC in transmodal regions (higher principal gradient) ($p < 0.001$). Responders primarily had higher SFC in unimodal regions and lower SFC in attentional networks (median principal gradient) ($p < 0.001$).

Conclusions. Our findings reveal opposing SFC alterations in low-level unimodal and high-level transmodal networks, underscoring spatial variability in MDD pathology. Moreover, hierarchy-specific antidepressant effects provide valuable insights into predicting treatment outcomes.

Introduction

Major depressive disorder (MDD) is a prevalent and debilitating public health problem, which has a 12-month prevalence of 6.6% and a lifetime prevalence of 16.2%, leading to a major decrease in quality of life (Kessler et al., 2007; Kupfer, Frank, & Phillips, 2012). The current treatment for MDD is only moderately successful. At least 50% of depressive patients respond to first-line treatment and recurrence (Rush et al., 2009; Thase et al., 2007). Thus, there is a pressing need to understand the neurobiology of MDD and its treatment response.

Neuroimaging works have provided important insights into MDD pathophysiology and antidepressant neuropharmacology. Findings from structural and functional imaging demonstrated that MDD may originate from disrupted interconnections among brain networks (Gong & He, 2015; Gudayol-Ferre, Pero-Cebollero, Gonzalez-Garrido, & Guardia-Olmos, 2015; Helm et al., 2018; Kaiser, Andrews-Hanna, Wager, & Pizzagalli, 2015; Mulders, van Eijndhoven, Schene, Beckmann, & Tendolkar, 2015). When detecting disrupted brain networks in MDD, there is also a great interest in elucidating the relationship between brain structure and function. Results concerning the relationship between structural and functional networks were heterogeneous (Scheepens et al., 2020). Specifically, whereas some studies reported increased patterns, others observed decreased patterns. Comparing the MDD patients to healthy individuals, studies reported a negative relationship between significant structural and functional measures involving subgenual anterior cingulate cortex (ACC) -hippocampus connectivity (de Kwaasteniet et al., 2013) and dorsal ACC and precuneus (Nixon et al., 2014). The decreased functional-structural coupling was also found in intra-hemispheric connections (Jiang et al., 2019) and feeder connections (Liu et al., 2020), which linked hub and non-hub

© The Author(s), 2024. Published by Cambridge University Press

regions. Conversely, a study reported the positive relationships between structural and functional measures spanning supragenual ACC (Spati et al., 2015). An increased structure-to-function correlation was observed in the prefrontal cortex (PFC) and ACC in patients with MDD (Scheinost et al., 2018). Thus, the relationship between structural and functional networks in MDD and its response to antidepressants remains unclear.

Critically, emerging evidence indicate that the structure-function relationship is not uniform in the brain. The divergence between structure and function was found to systematically follow a functional hierarchy, spanning from low-level modality-specific unimodal regions to high-level function-diverse transmodal regions (Vazquez-Rodriguez et al., 2019). According to functional specialization, the brain regions can be categorized into unimodal regions and transmodal regions. Specifically, unimodal regions, including primary sensory and motor cortices, specialize in processing information from single sensory modalities or functions (Braga, Sharp, Leeson, Wise, & Leech, 2013; Margulies et al., 2016). Transmodal regions, also known as heteromodal, paralimbic, or multiple association regions, are involved in integrating information from multiple functional networks (Margulies et al., 2016). Unimodal regions exhibit a close alignment between structure and function, while transmodal regions exhibit divergent structure-function relationships (Baum et al., 2020; Vazquez-Rodriguez et al., 2019). In conclusion, structure-function couplings (SFC) do not relate in exactly the same way across the whole brain but potentially converges or diverges following functional hierarchy. Therefore, exploring SFC should consider corresponding spatial variations across the whole brain.

The gradient mapping technique introduces a novel way to measure the functional hierarchy continuously, known as the functional gradient. This gradient is closely linked with the coupling between structure and function (Huntenburg, Bazin, & Margulies, 2018; Margulies et al., 2016). Furthermore, this coupling varies spatially across the brain, aligning with the functional gradient in healthy individuals. This variation extends from sensory networks to the default mode network (DMN), illustrating a spectrum of connectivity (Preti & Van De Ville, 2019; Vazquez-Rodriguez et al., 2019). Therefore, the functional gradient in healthy individuals demonstrates the disproportionately distributed SFC along with the unimodal-transmodal axis. In patients with MDD, whether such disproportionate distribution of SFC would enhance or disappear is worthy to explore. Furthermore, how abnormal SFC indicates treatment outcomes is also useful for precision treatment.

Here, we aimed to explore altered SFC in MDD and its indications on antidepressant treatment from a hierarchical perspective. Here, we hypothesized that the abnormality of SFC in MDD exhibited multiple patterns from low-level primary sensory cortex to high-level association cortex and such abnormality would be indicative of treatment response.

Methods

Sample

Participants enrollment

All participants received diffusion tensor imaging (DTI), resting-state functional magnetic resonance imaging (MRI) and mental evaluations at baseline from the Affiliated Brain Hospital of Nanjing Medical University. They were provided with a complete description of the study before signing written informed consent forms. The Research Ethics Review Board of the Affiliated Brain Hospital of Nanjing Medical University approved the study, ensuring compliance with ethical standards of national and institutional committees on human experimentation and the Helsinki Declaration of 1975, as revised in 2008. Figure 1 presents the study design for participant enrollment.

Patients with MDD were diagnosed according to the Diagnostic and Statistical Manual of Mental Disorders, Fourth Edition (DSM-IV), and their depressive severities were evaluated using 17-item Hamilton Rating Scale for Depression (HAMD). The inclusion criteria for patients included: (1) a 17-item HAMD score above 17; (2) ages 18 to 55 years; (3) no antidepressants or stimulation therapy in the two weeks preceding baseline recruitment. Exclusion criteria for patients included: (1) current pregnancy or breastfeeding; (2) any contraindications to MRI scanning; (3) serious medical or neurological illnesses, including severe somatic diseases and organic brain disorders; (4) acute homicidal or suicidal tendencies; (5) substance dependence/abuse within the past year.

Healthy controls were (HC) assessed using the non-patient version of the MINI Structured Clinical Interview for DSM-IV, Chinese version. Inclusion criteria for HC included: (1) ages 18 to 55 years; (2) no family history of psychiatric disorders in first-degree relatives; (3) no history of psychotropic medication use. Exclusion criteria for HC were: (1) substance dependence or abuse, neurological illness; (2) contraindications to MRI scans.

Participants for exploring treatment response

To explore the effect of SFC in predicting antidepressant response, patients were further screened as a treatment group according to the following inclusion criteria: (1) received the selective serotonin-reuptake inhibitors (SSRIs) monotherapy or (2) selective serotonin–noradrenaline reuptake inhibitors (SNRIs) monotherapy. The exclusion criteria of the treatment group contained: The exclusion criteria of the treatment group contained: (1) having received any form of stimulation therapy, such as electroconvulsive therapy (ECT) or repetitive transcranial magnetic stimulation (rTMS); (2) having experienced a manic or hypomanic episode; (3) being lost to follow-up; (4) using a combination of two types of antidepressants; (5) changing to another type of antidepressant.

Patients were prescripted by two attending psychiatrists according to their symptoms and possible side effects of antidepressants. All patients were treated with flexible antidepressant doses that followed corresponding medication guidelines and would be altered depending on the illness conditions. Depressive symptom severity was measured using 17-item HAMD (HAMD-17). The primary outcome measure was a decrease in HAMD-17 scores in 6-week follow-up. The reduction in HAMD-17 was defined as the changed percentage of HAMD between the baseline and the end of follow-up. Responders were patients who achieved the clinical response, which was defined as a reduction in HAMD of 50% or more from baseline (Henkel et al., 2009).

Participants for the principal gradient definition

To obtain a reliable and convincing functional hierarchical organization, we calculated the principal gradient using samples from Human Connectome Projects (HCP) (Van Essen et al., 2013). 217 healthy individuals (56.22% female, mean + S.D. age, 28.5 ± 3.7 years) were included. The resting-state functional MRI and structural imaging were completed by HCP. There were no family relationships between each two of the samples. The details of

https://doi.org/10.1017/S0033291724000801 Published online by Cambridge University Press

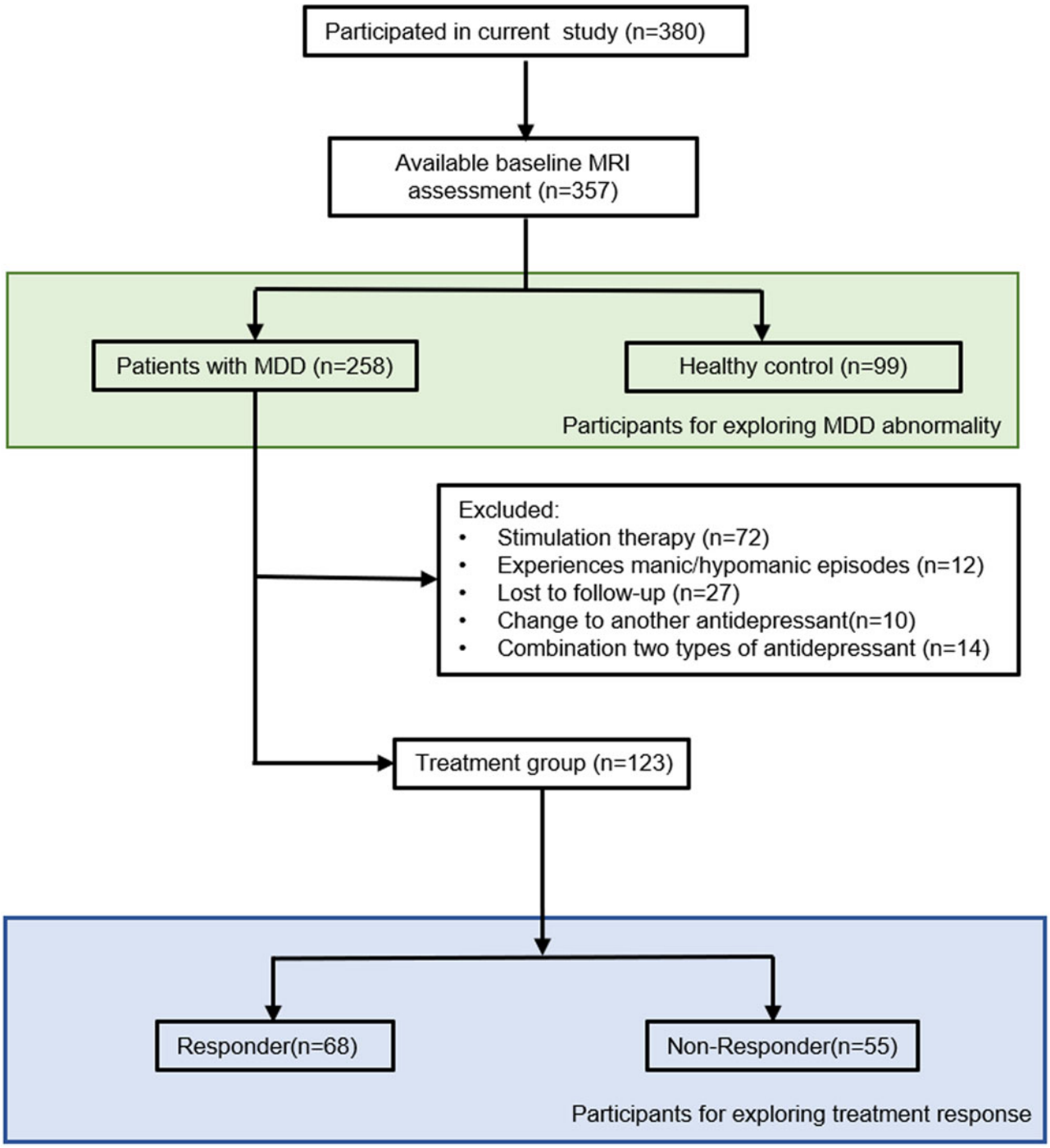


Figure 1. The participant's enrollment and selection. Abbreviation: ECT: electroconvulsive; rTMS: repetitive transcranial magnetic stimulation.

subjects inclusion and processing approach can be found in the prior publication (Reinder et al., 2018). Accordingly, informed consent was approved by the Washington University institutional review board.

MRI acquisition and processing

All MRI data were collected from the Affiliated Brain Hospital using 3T Siemens Verio scanner (Erlangen, Germany) with an 8-channel radiofrequency coil. There were three imaging sequences: DTI, resting-state functional MRI, and T1-weight imaging. Parameters for T1-weight axial images were: repetition time/echo time (TR/TE) = 1900/2.48 ms, flip angle = 9°, matrix = 256 × 256, field of view (FOV) = 250 mm × 250 mm, and slice = 176. The DTI were acquired with the following parameters: TR/TE = 6600/93 ms, matrix = 128 × 128, FOV = 240 mm × 240 mm, slice = 45, flip angle = 90°. And the resting-state functional MRI data were obtained using the parameters as follows: TR/TE = 3000 ms/40 ms, FOV = 240 mm × 240 mm, flip angle = 90°, 32 slices with slice thickness = 4 mm without gap,

https://doi.org/10.1017/S0033291724000801 Published online by Cambridge University Press

matrix size = 64 × 64, and 133 volumes, voxel size = 3.75 × 3.75 × 4 mm^3. For resting-state functional MRI data, frame-wise motion parameters were calculated using six rigid motion parameters. Subjects whose translations were greater than 2 mm or whose rotations were greater than 2° were excluded.

The DTI pre-processing was performed with the diffusion toolbox of Functional Magnetic Resonance Imaging of the Brain (FMRIB) software library (FSL, http://fsl.fmrib.ox.ac.uk/fsl/fslwiki/). Firstly, we corrected eddy-current-induced distortion and head movements. Then, we striped the brain skull and extract the brain tissue, providing better alignment results and reducing the computational time by excluding non-brain tissue. The eddy current distortions and motion artifacts were corrected by applying a rigid body transformation from each diffusion-weighted image to the b0 image. The diffusion tensor matrix was calculated according to Stejskal and Tanner equation [30]. By diagonalization of the tensor matrix, three eigenvalues and eigenvectors were obtained. Then, fractional anisotropy (FA) maps were estimated. Each DTI image was registered to the T1-weighted image and then to the MNI-152 space. Three-dimensional fiber tract reconstruction was implemented by DiffusionKit toolbox (http://diffusion.brainnetome.org/). Whole-brain tractography was obtained using the Fiber Assignment by Continuous Tracking (FACT) algorithm. The fiber tracking procedures were terminated when a voxel was encountered with FA below 0.2 or a minimum angle was larger than 50°.

We preprocessed resting-state MRI data through SPM8 (www.fil.ion.ucl.ac.uk/spm/software/spm8) and REST toolbox (www.restfmri.net). We removed the first six functional volumes to exclude the T1 saturation effect. Subsequently, we employed slice-timing correction and head-motion correction for all the remaining images. Images were then co-registered to the corresponding high-resolution T1 anatomical images which were transformed into the Montreal Neurological Institute (MNI) space. Afterwards, functional images were resampled to 3 × 3 × 3 mm^3 voxels, smoothed with a 6-mm-full-width, half-maximum Gaussian kernel. Linear detrending and temporal band-pass filtering (0.01–0.08 Hz) were performed. Motion parameters, white matter, and cerebral signal fluid were regressed out from the time series at subject level.

Brain network construction and SC-FC coupling calculation

We generated the whole-brain structural and functional networks for each individual, based on the Schaefer 7-network atlas with 400 parcels (Schaefer et al., 2018). Eighteen additional subcortical structures from the Automatic Anatomical labeling (AAL) (Tzourio-Mazoyer et al., 2002) were added to the parcellation, resulting in 418 total regions (Additional subcortical structure shown in online Supplementary Table S1).

Structural connectivity (SC) of structural networks was white matter projections, which were defined by the mean FA across streamlines between two brain regions. Two regions were anatomically connected if at least two fibers whose fiber length was greater than 10 mm passed through these two regions. We defined the weight of structural connectivity as the mean FA value along all fibers connecting two nodes. Edges of functional networks were functional connectivity (FC) which was defined as the *z*-transformed *Pearson* correlation coefficient between regional time series.

Here, we calculated the coupling between structural and functional connectivity (SC-FC coupling) by focusing on the regional connectivity profiles, using the *Spearman* rank correlation between regional connectivity profiles of structural and functional networks. For each participant, regional connectivity profile was represented as the vector of strength from a single region to the rest of regions in the whole-brain. Specifically, the regional connectivity profile was extracted from each row of the network adjacent matrix. Non-zero structural connections weights were isolated and further rescaled into a Gaussian distribution (Koubiyr et al., 2019; Nabulsi et al., 2020). The corresponding FC was extracted and correlated with its structural counterparts, resulting 418 regional SC-FC coupling values for each participant.

Extraction of maps for principal resting-state FC gradients

To denote the position of node on the functional hierarchical axis, we calculated the gradient score for each region. The diffusion map embedding method (Coifman & Lafon, 2006) was used to identify principal gradient components using BrainSpace toolbox (Vos de Wael et al., 2020) (https://github.com/MICA-MNI/BrainSpace). A group-averaged functional connectivity matrix was constructed, thresholded, normalized, decomposed via the diffusion embedding method. To obtain the reliable and interpretable gradient, we only taken the gradient component with the highest variance, named as principal gradient.

Statistical analysis

For demographic information, two-sample *t* tests and χ^2 tests were used to assess group differences (MDD *v.* HC, Responders *v.* Non-responders) in demographic variables. Differences of gender were assessed by the χ^2 tests, while age and education were assessed by two-sample *t* tests.

To explore MDD disruptions in SC-FC coupling, we compared regional coupling values between HC and patients with MDD. The normal distribution of SC-FC coupling values was measured by the Shapiro–Wilk test. Then, the independent two-sample *t* test and the Mann-Whitney test were used to compare group differences depending on above data normality, respectively. We employed false discovery rate (FDR) correction with $p < 0.05$. To explore how the SC-FC coupling referred to treatment outcomes, we also compared regional coupling values between responders and non-responders. The group comparison followed the same procedure as the MDD disruptions detection.

After we identified regions showing group differences, we investigated how these altered and response-associated SC-FC couplings varied across principal gradient. We firstly ranked the eight functional networks according to their functional networks. Then, we categorized significantly different regions into their corresponding networks, and evaluated their differences using effect sizes (Cohen's d).

Results

Sample

From the 380 participants initially enrolled, 23 were excluded due to incomplete MRI scans or poor data quality. This resulted in a study cohort of 258 patients diagnosed with MDD and 99 HC. The MDD group comprised 142 females (55.04%), with an average age of 31.78 years (S.D. = 12.03), an education level of 13.66 years (S.D. = 3.02), a disease duration of 5.65 months (S.D. = 9.43), and a baseline HAMD score of 22.58 (S.D. = 6.19). The

https://doi.org/10.1017/S0033291724000801 Published online by Cambridge University Press

Table 1. Demographic and treatment administrations for the treatment group

	Responders	Non-responders	*p*
Number	68	55	
Gender	28/40	26/29	0.498[a]
Age (year)	32.22 ± 10.83	31.64 ± 11.56	0.778[b]
Years of education	13.42 ± 5.07	13.38 ± 4.49	0.959[b]
HAMD-17 (baseline)	23.08 ± 5.72	23.84 ± 4.93	0.47[b]
SSRIs (sample number)	49	42	
Escitalopram (mg/day)	19.2 ± 1.9	17.8 ± 3.6	
Sertraline (mg/day)	82.4 ± 35.7	90.2 ± 28.7	
SNRIs (sample number)	19	13	
Venlafaxine (mg/day)	172.5 ± 35.4	143.3 ± 28	
Duloxetine (mg/day)	74.7 ± 26	68.2 ± 21	

[a]The *p* value was obtained by χ^2 tests.
[b]The *p* value was obtained by two-sample *t* tests.
Abbreviations: HAMD-17: 17-item Hamilton Rating Scale for Depression.

HC group included 51 females (51.52%), with an average age of 31.83 years (S.D. = 8.49) and an education level of 14.22 years (S.D. = 2.59). Analyses revealed no significant differences in gender, age, or education level between MDD patients and HC.

For the exploration of treatment response, 123 of the 258 MDD patients were further selected and categorized into 68 responders and 55 non-responders. Among these 123 patients, 91 received SSRIs and 32 received SNRIs. The demographic, clinical variables, and treatment details of the patients in the treatment group are presented in Table 1.

Principal gradient across the whole brain

The principal gradient accounted for 27.59% of variances and showed functional differentiation from visual and sensorimotor networks to DMN. The principal gradient was showed in Fig. 2a. The regional principal gradient value reflects the position of regions in the principal gradient axis and indicates its similarity of connectivity profiles with the gradient axis. The eight functional networks were ranked by the increase of principal gradient values as following (Fig. 2b): visual network (VIS), sensorimotor network (SMN), dorsal attention network (DAN), ventral attention network (VAN), subcortical network (SUB), limbic network (LIB), frontparietal network (FPN), DMN. The networks with lower principal values were named unimodal networks, while those with higher principal values were named transmodal networks.

SC-FC coupling in MDD changed along with the principal gradient

Comparing patients of MDD with HC, we found 30 significantly different regions, spanning eight networks. Fig 2c presented the significant regions with increased (red) and decreased (blue) SC-FC coupling in MDD patients ($p < 0.001$). To investigate the abnormal regional distribution along with the principal gradient, we categorized significant regions into their corresponding networks (Fig. 2d). We observed two abnormal patterns: the increased patterns in low-level unimodal networks and decreased patterns in high-level transmodal networks in patients with MDD. Specifically, compared to HC, patients with MDD showed increased SC-FC coupling in unimodal regions, spanning VIS, SMN, DAN, and VAN. In contrast, patients with MDD had decreased SC-FC coupling in high-level transmodal networks, involving SUB, LIB, FPN. Particularly, DMN was a unique network that showed both increased and decreased group-differences. Specifically, major part of DMN exhibited increased SC-FC couplings in MDD, while the left medial prefrontal cortex (mPFC) showed a decreased SC-FC coupling.

SC-FC coupling regarding antidepressant response along with the principal gradient

We found nine regions showing significant differences between responders and non-responders, spanning over VIS, SMN, DAN, VAN, FPN, and DMN (Fig. 3a). Compared to non-responders, responders had higher SC-FC couplings in VIS (left cuneus, $p < 0.001$), SMN (left precentral gyrus, $p < 0.001$), FPN (right ACC, $p < 0.001$) and lower SC-FC couplings in DAN (left middle temporal gyrus (MTG), $p < 0.001$) and VAN (left superior temporal gyrus (STG), $p < 0.001$) (Fig. 3b and c). Similarly, DMN also exhibited two directional differences. Specifically, in responders, posterior DMN showed increased coupling spanning left precuneus ($p < 0.001$) and posterior cingulate cortex (PCC) ($p < 0.001$), while anterior DMN showed decreased SC-FC couplings in left mPFC ($p < 0.001$) and right mPFC ($p < 0.001$)) (Fig. 3d).

Discussion

We characterize SFCs in MDD and their antidepressant specificity by spatial hierarchy. We found hierarchy-specific SC-FC disturbances in MDD and antidepressant response, which suggested spatial variability in MDD pathology and it could infer treatment outcomes. As SC-FC coupling in healthy populations has been proven to distribute disproportionately across the unimodal-transmodal axis (Preti & Van De Ville, 2019; Vazquez-Rodriguez et al., 2019), we found that such disproportionate distribution was enhanced in MDD. Among MDD patients, we further inferred that patients with increasingly disproportionate distributions were more sensitive to antidepressants. The findings supported antidepressant response prediction and provided the potential mechanism of antidepressant efficacy.

https://doi.org/10.1017/S0033291724000801 Published online by Cambridge University Press

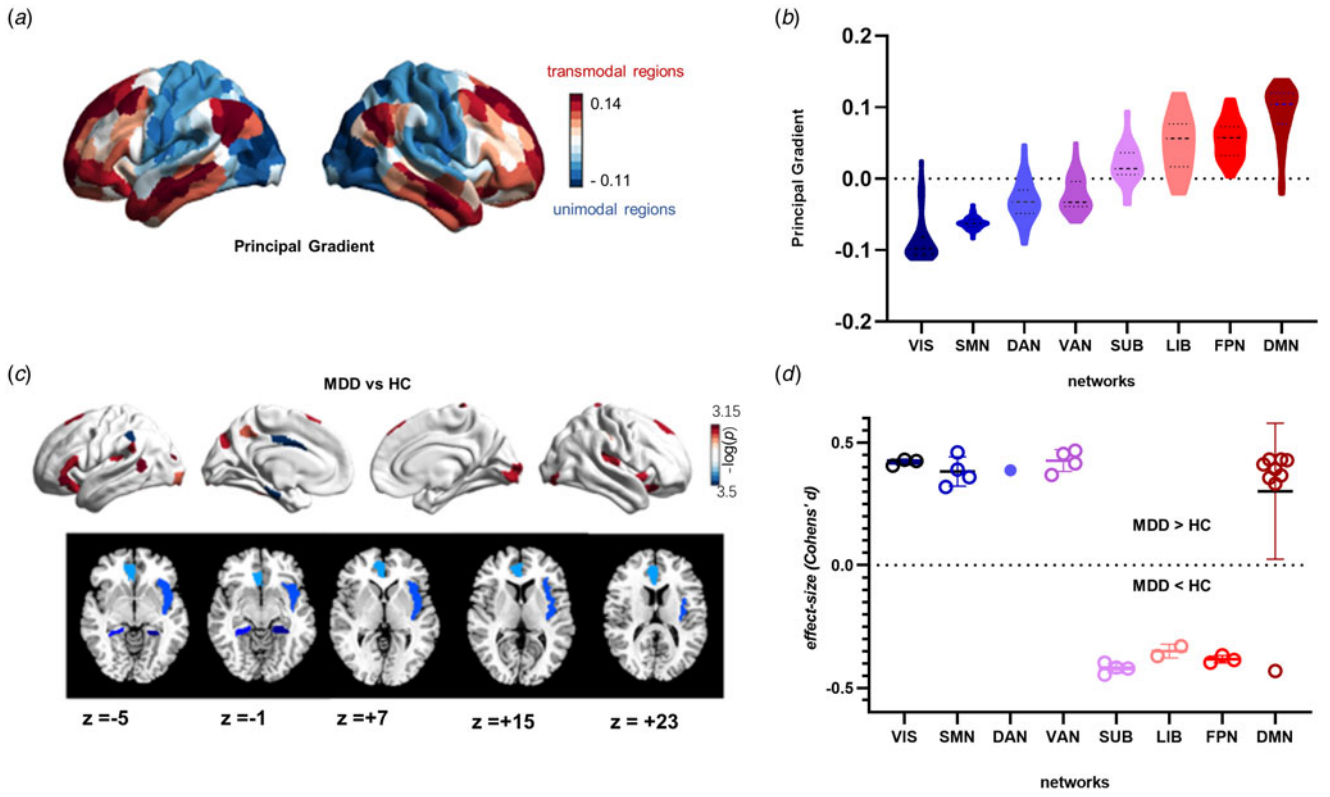


Figure 2. Principal gradients and regions with significant differences in SC-FC coupling for MDD disruptions. (a) The principal gradient spanning the whole brain. (b) Violin plot of the principal gradients across eight functional networks. (c) Regions showing significant differences in SC-FC coupling between patients with MDD and healthy controls. The colorbar is −log10 transformed *p* value, where red indicates the higher coupling and blue indicates the lower coupling in MDD patients. (d) Scatter dot plot of effect sizes (Cohen's d) (*MDD minus HC*) for abnormal patterns between patients with MDD and healthy controls among eight functional networks. Each dot indicates a significant region within the corresponding network. The error bar is the standard deviation. Different colors indicate different networks corresponding to Fig. 2b.

Pathology of MDD in SC-FC coupling

For MDD pathology, patients with MDD had higher SFC in low-level unimodal regions, while lower SFC was observed in transmodal regions, except for DMN. The SC-FC coupling reflects how white matter pathways support functional communication (Suarez, Markello, Betzel, & Misic, 2020). Increased SC-FC coupling values suggest a strong correlation between white matter pathways and functional synchrony, implying that functional communication is directly dependent on local white matter pathways (Vazquez-Rodriguez et al., 2019). Conversely, reduced SC-FC coupling reflects functional flexibility, where functional communications are not bound by structural constraints (Baum et al., 2020). Therefore, the observed variations in SC-FC coupling in MDD, including both enhancements and reductions, suggest that the disease impacts brain communication patterns in distinct ways across unimodal and transmodal regions.

Specifically, in the primary sensory and visual areas, we found a higher correlation between structure and function in MDD. It suggested that functional communications in these regions were more likely to rely on the status of local white-matter pathways (Preti & Van De Ville, 2019). In contrast to transmodal regions, the primary visual and sensory regions have more stable structural configurations, which stems from their highly myelinated associations and stronger laminar differentiation (Paquola et al., 2019). Accordingly, the stronger interaction between structure and function would reduce functional flexibility and promote more segregated functional systems. That is why some studies reported low functional activity of these regions in MDD. The reduced functional connectivity between SMN and VIS and low neuronal variability of SMN and VIS were also reported (Zhao et al., 2021). These stemmed from the fact that the more constrained functional connectivity always indicated more stringent and less dynamic brain function (van den Heuvel et al., 2013). In summary, MDD exposure leads to enhanced structural rigidity and diminished functional communication in the brain, thereby reinforcing SC-FC correlations.

In the transmodal regions, decreased correlations between structural pathways and functional connectivity were observed, which was consistent with previous findings in other brain diseases. Specifically, such structure-function decoupling was also found in bipolar disorders (Jiang et al., 2020), schizophrenia (Cocchi et al., 2014), Alzheimer's disease (Dai et al., 2019), epilepsy (Zhang et al., 2011), and stroke (Zhang et al., 2017). Given that transmodal cortices receive and process signals originating from multiple sources across the network, they always have the high ability for functional diversity and cognitive flexibility [21]. Also, the richer local cytoarchitecture in transmodal cortex supports increasingly autonomous and spontaneous dynamics of function (Shafiei et al., 2019), leading to more untethered functional communications. Since regions in FPN and LIB present high values and high costs in integrating information and intermodular communication, they are more vulnerable to pathogenic processes (Crossley et al., 2014). Thus, decreased SC-FC coupling in MDD is caused by its

https://doi.org/10.1017/S0033291724000801 Published online by Cambridge University Press

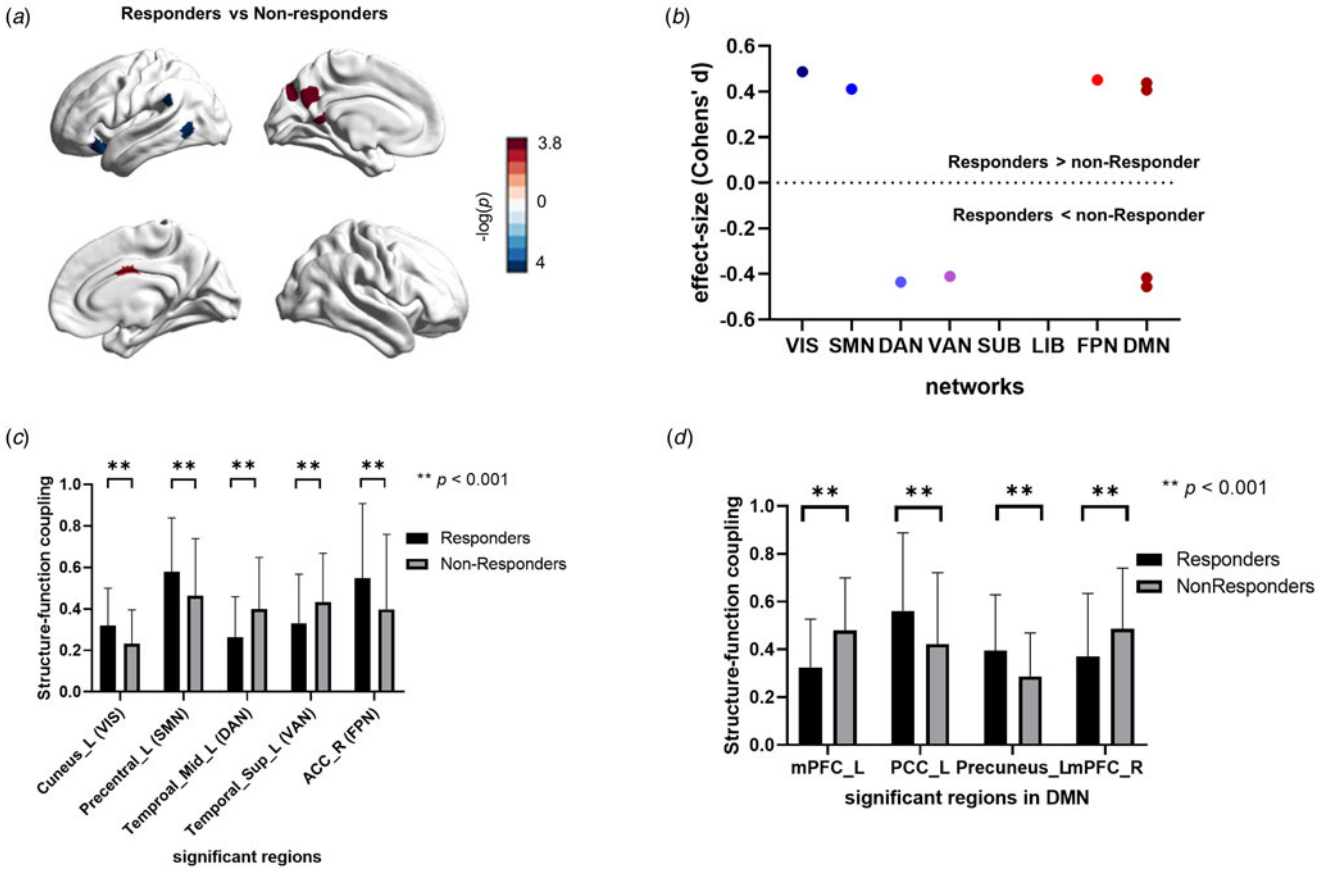


Figure 3. Regions showing significant difference in SC-FC coupling between responders and non-responders. (a) Cortical surface rendering showing regional significant differences in SC-FC coupling between responders and non-responders. The color indicates −log10 (*p* value), where red indicates the higher coupling in responders and blue indicates the lower coupling. (b) Scatter dot plot of effect sizes (Cohen's d) (*Responders minus non-Responders*) in SC-FC coupling. Each dot indicates a significant region within the corresponding network. The error bar is the standard deviation. (c) Bar plot of significant nodes in VIS, SMN, DAN, VAN and FPN. (d) Bar plot of significant regions in DMN. Abbreviations: Cuneus_L: left cuneus; Precentral_L: left precentral gyrus; Temporal_Mid_L: middle temporal cortex; Temporal_Sup_L: superior temporal cortex; mPFC_L/mPFC_R: left/right medial prefrontal cortex; PCC_L: left posterior cingulate cortex.

functional vulnerability. Given the important role of these regions in emotional regulations and cognition controls, we speculate that less constrained functional communications of FPN and LIB may represent reduced structural capacity to integrate information, leading to the observed emotional symptoms and cognitive deficits.

Effect of SC-FC coupling on antidepressant response

Consistent with observations of MDD disruption, SFC also displayed bidirectional variations, extending from unimodal to transmodal regions. Our findings revealed that baseline patients exhibiting higher coupling in the visual and sensorimotor regions, the ACC, and the posterior DMN, alongside lower coupling in the superior and middle temporal gyrus and anterior DMN, were associated with improved antidepressant outcomes.

As discussed previously, the visual and sensorimotor regions exhibited enhanced structural network configurations and diminished functional communications in response to disease attacks. Consequently, the elevated SC-FC coupling observed in unimodal regions suggested a stable state that may be beneficial in counteracting these attacks. In individuals responding to treatment, this heightened state of stability within the visual and sensorimotor networks is believed to preserve basic functions, thereby contributing to more favorable outcomes. In contrast, the ACC, lacking strong structural profiles but exhibiting high SC-FC coupling in responders, plays a pivotal role in serotonergic neurotransmission modulation. ACC neurons receive serotonergic innervation from the raphe nuclei and neuromodulatory input from locus coeruleus noradrenaline neurons, enhancing serotonin transporter availability post-SSRI treatment, which may boost neurotransmission and antidepressant efficacy (Koga et al., 2020; Tian, Yamanaka, Bernabucci, Zhao, & Zhuo, 2017). The serotonin transporter availability was also found to increase in ACC after SSRI treatment (James et al., 2017). Thus, increased SC-FC coupling in the ACC, indicative of enhanced serotonergic modulation, alongside stable couplings in visual and sensorimotor regions, correlates with improved treatment outcomes.

STG and MTG show lower SC-FC coupling in responders, correlating with diminished functional and structural profiles. Decreased FC in the STG for sertraline responders and in the MTG for venlafaxine responders was observed (Tozzi, Goldstein-Piekarski, Korgaonkar, & Williams, 2020), along with smaller gray matter volume in MTG post-treatment remitters and reduced metabolism in the STG among antidepressant responders (Fonseka, MacQueen, & Kennedy, 2018). These findings suggest that reduced structural and functional integrity in STG and MTG is associated with a positive treatment response.

https://doi.org/10.1017/S0033291724000801 Published online by Cambridge University Press

Bidirectional differences of DMN

An interesting phenomenon was found for DMN in MDD and treatment response. Contrary to networks showing unidirectional changes, DMN exhibited both increased and decreased SC-FC coupling. Importantly, increased coupling was observed in the posterior DMN, associated with responders, while decreased coupling characterized the anterior DMN. This bifurcation suggests differential roles of DMN's anterior and posterior segments in mediating treatment outcomes.

Previous studies highlight DMN's uniqueness in SC-FC coupling. Baum et al., reported strong coupling in the mPFC, a central DMN hub, contrasting with looser coupling in other transmodal regions (Baum et al., 2020). Osmanlıoglu et al., found DMN's high structure-function congruence, akin to visual and motor systems (Osmanlioglu et al., 2019), might relying on its functional flexibility and dynamic recruitment during diverse task demands (Yeo et al., 2016). When referring to antidepressant responses, the particularity of DMN was attributable to differences in DMN subsystems in antidepressant effects.

Anterior DMN implicates in self-referential thought, whereas posterior DMN's play a important role in sensory processing and memory (Qin et al., 2012; Whitfield-Gabrieli et al., 2011). The posterior DMN, sharing functional similarities with sensory and motor areas, shows increased SC-FC coupling in responders, indicating structural stability conducive to antidepressant effects. Antidepressants primarily normalize alterations in the posterior DMN (Li et al., 2013), suggesting that baseline higher structural support in this area facilitates the normalization process in responders. Conversely, the anterior DMN's abnormalities remain unaltered by antidepressants, with its enhanced self-referential activity linked to MDD's rumination aspect. Increased anterior DMN activity during rumination has been consistently documented (Zhou et al., 2020), with dopamine differentially influencing the anterior and posterior DMN hubs (Knyazev, 2012). Thus, previous studies suggested that antidepressants modulated enhanced activations of self-referential processing which was mainly involved in anterior DMN. We suspect that antidepressants target the heightened self-referential processes of the anterior DMN, positing that lower SC-FC coupling here may allow greater functional flexibility, aiding inhibition processes. Thus, individuals with structurally supported posterior DMN and flexible anterior DMN functions are likely to benefit more from antidepressant treatments.

Several limitations of our study were noteworthy. First, it employs the principal gradient value as a categorical marker rather than a continuous variable to define regions along the visual-transmodal axis, necessitating future research to explore the gradient scores' statistical correlation with brain impairments. Secondly, being cross-sectional, our study has limited capability in generalizing treatment response findings. Lastly, the use of both the two-sample *t* test and the Mann-Whitney test introduces methodological variability, potentially impacting result validity. Future efforts will aim to expand the participant base to strengthen the research outcomes.

In conclusion, our study provided a hierarchical perspective of SFC in MDD and its correlation with antidepressant response. The findings suggest that MDD leads to enhanced brain communications in unimodal regions and the posterior DMN, but reduced in transmodal areas. Importantly, patients with stronger anatomical support in unimodal and posterior DMN regions, along with more adaptable attention and anterior DMN networks, are more responsive to antidepressants. This highlights the potential for using hierarchical changes in structure-function relationships to predict antidepressant responses in future research.

Supplementary material. The supplementary material for this article can be found at https://doi.org/10.1017/S0033291724000801.

Data availability statement. The data and codes supporting this study's findings are available on request from the corresponding author. The raw neuroimaging data are not publicly available due to privacy or ethical restrictions.

Acknowledgements. We would like to express our gratitude to all the participants in the Affiliated Brain Hospital of Nanjing Medical University.

Authors' contributions. **X. W.:** Conceptualization, Methodology, Visualization, Software, Results interpretation, Writing-Original Draft and Revision, Final approval of the version to be published **L. X.:** Methodology, Software; **L. H.:** Results interpretation; **J. S.:** Software, Visualization; **R. Y.:** Data acquisition; **Z. Y.:** Project administration, Data acquisition, **Q. L.:** Conceptualization, Revising the work, Final approval of the version to be published.

Funding statement. The work was supported by the National Natural Science Foundation of China (82151315, 82271568, 82101573, 82301718); Jiangsu Medical Innovation Center for Mental Illness (CXZX202226); Jiangsu Provincial Key Research and Development Program (BE2019675); Key Project of Science and Technology Innovation for Social Development in Suzhou (2022SS04); Jiangsu Provincial Natural Science Youth Fund (BK20230154); Key Project supported by Medical Science and Technology Development Foundation, Nanjing Commission of Health (ZKX21035); General project of Nanjing Science and Technology Development Plan (YKK22140); the Fundamental Research Funds for the Central Universities (2242021k30014).

Competing interests. None.

Ethical standards. The authors assert that all procedures contributing to this work comply with the ethical standards of the relevant national and institutional committees on human experimentation and with the Helsinki Declaration of 1975, as revised in 2008.

References

Baum, G. L., Cui, Z., Roalf, D. R., Ciric, R., Betzel, R. F., Larsen, B., … Satterthwaite, T. D. (2020). Development of structure-function coupling in human brain networks during youth. *Proceedings of the National Academy of Sciences of the United States of America*, *117*(1), 771–778. https://doi.org/10.1073/pnas.1912034117

Braga, R. M., Sharp, D. J., Leeson, C., Wise, R. J. S., & Leech, R. (2013). Echoes of the brain within default mode, association, and heteromodal cortices. *The Journal of Neuroscience*, *33*, 14031–14039.

Cocchi, L., Harding, I. H., Lord, A., Pantelis, C., Yucel, M., & Zalesky, A. (2014). Disruption of structure-function coupling in the schizophrenia connectome. *NeuroImage: Clinical*, *4*, 779–787. https://doi.org/10.1016/j.nicl.2014.05.004

Coifman, R. R., & Lafon, S. (2006). Diffusion maps. *Applied and Computational Harmonic Analysis*, *21*(1), 5–30. https://doi.org/10.1016/j.acha.2006.04.006

Crossley, N. A., Mechelli, A., Scott, J., Carletti, F., Fox, P. T., McGuire, P., & Bullmore, E. T. (2014). The hubs of the human connectome are generally implicated in the anatomy of brain disorders. *Brain*, *137*(Pt 8), 2382–2395. https://doi.org/10.1093/brain/awu132

Dai, Z., Lin, Q., Li, T., Wang, X., Yuan, H., Yu, X., … Wang, H. (2019). Disrupted structural and functional brain networks in Alzheimer's disease. *Neurobiology of Aging*, *75*, 71–82. https://doi.org/10.1016/j.neurobiolaging.2018.11.005

de Kwaasteniet, B., Ruhe, E., Caan, M., Rive, M., Olabarriaga, S., Groefsema, M., … Denys, D. (2013). Relation between structural and functional

connectivity in major depressive disorder. *Biological Psychiatry*, *74*(1), 40–47. https://doi.org/10.1016/j.biopsych.2012.12.024

Fonseka, T. M., MacQueen, G. M., & Kennedy, S. H. (2018). Neuroimaging biomarkers as predictors of treatment outcome in major depressive disorder. *Journal of Affective Disorders*, *233*, 21–35. https://doi.org/10.1016/j.jad.2017.10.049

Gong, Q., & He, Y. (2015). Depression, neuroimaging and connectomics: A selective overview. *Biological Psychiatry*, *77*(3), 223–235. https://doi.org/10.1016/j.biopsych.2014.08.009

Gudayol-Ferre, E., Pero-Cebollero, M., Gonzalez-Garrido, A. A., & Guardia-Olmos, J. (2015). Changes in brain connectivity related to the treatment of depression measured through fMRI: A systematic review. *Frontiers in Human Neuroscience*, *9*, 582. https://doi.org/10.3389/fnhum.2015.00582

Helm, K., Viol, K., Weiger, T. M., Tass, P. A., Grefkes, C., Del Monte, D., & Schiepek, G. (2018). Neuronal connectivity in major depressive disorder: A systematic review. *Neuropsychiatric Disease and Treatment*, *14*, 2715–2737. https://doi.org/10.2147/NDT.S170989

Henkel, V., Seemüller, F., Obermeier, M., Adli, M., Bauer, M., Mundt, C., … Riedel, M. (2009). Does early improvement triggered by antidepressants predict response/remission? Analysis of data from a naturalistic study on a large sample of inpatients with major depression. *Journal of Affective Disorders*, *115*(3), 439–449. https://doi.org/10.1016/j.jad.2008.10.011

Huntenburg, J. M., Bazin, P. L., & Margulies, D. S. (2018). Large-scale gradients in human cortical organization. *Trends in Cognitive Sciences*, *22*(1), 21–31. https://doi.org/10.1016/j.tics.2017.11.002

James, G. M., Baldinger-Melich, P., Philippe, C., Kranz, G. S., Vanicek, T., Hahn, A., … Lanzenberger, R. (2017). Effects of selective serotonin reuptake inhibitors on interregional relation of serotonin transporter availability in major depression. *Frontiers in Human Neuroscience*, *11*, 48. https://doi.org/10.3389/fnhum.2017.00048

Jiang, H., Zhu, R., Tian, S., Wang, H., Chen, Z., Wang, X., … Lu, Q. (2020). Structural-functional decoupling predicts suicide attempts in bipolar disorder patients with a current major depressive episode. *Neuropsychopharmacology*, *45*(10), 1735–1742. https://doi.org/10.1038/s41386-020-0753-5

Jiang, X. Y., Shen, Y. D., Yao, J. S., Zhang, L., Xu, L. Y., Feng, R., … Wang, J. H. (2019). Connectome analysis of functional and structural hemispheric brain networks in major depressive disorder. *Translational Psychiatry*, *9*(1), 136. https://doi.org/10.1038/s41398-019-0467-9

Kaiser, R. H., Andrews-Hanna, J. R., Wager, T. D., & Pizzagalli, D. A. (2015). Large-scale network dysfunction in major depressive disorder: A meta-analysis of resting-state functional connectivity. *JAMA Psychiatry*, *72*(6), 603–611. https://doi.org/10.1001/jamapsychiatry.2015.0071

Kessler, R. C., Angermeyer, M., Anthony, J. C., De Graaf, R., Demyttenaere, K., Gasquet, I., … Ustun, T. B. (2007). Lifetime prevalence and age-of-onset distributions of mental disorders in the World Health Organization's World Mental Health Survey Initiative. *World Psychiatry*, *6*(3), 168–176.

Knyazev, G. G. (2012). Extraversion and anterior vs. posterior DMN activity during self-referential thoughts. *Frontiers in Human Neuroscience*, *6*, 348. https://doi.org/10.3389/fnhum.2012.00348

Koga, K., Yamada, A., Song, Q., Li, X. H., Chen, Q. Y., Liu, R. H., … Chen, T. (2020). Ascending noradrenergic excitation from the locus coeruleus to the anterior cingulate cortex. *Molecular Brain*, *13*(1), 49. https://doi.org/10.1186/s13041-020-00586-5

Koubiyr, I., Besson, P., Deloire, M., Charre-Morin, J., Saubusse, A., Tourdias, T., … Ruet, A. (2019). Dynamic modular-level alterations of structural-functional coupling in clinically isolated syndrome. *Brain*, *142*(11), 3428–3439. https://doi.org/10.1093/brain/awz270

Kupfer, D. J., Frank, E., & Phillips, M. L. (2012). Major depressive disorder: New clinical, neurobiological, and treatment perspectives. *The Lancet*, *379*(9820), 1045–1055. https://doi.org/10.1016/s0140-6736(11)60602-8

Li, B., Liu, L., Friston, K. J., Shen, H., Wang, L., Zeng, L. L., & Hu, D. (2013). A treatment-resistant default mode subnetwork in major depression. *Biological Psychiatry*, *74*(1), 48–54. https://doi.org/10.1016/j.biopsych.2012.11.007

Liu, X., He, C., Fan, D., Zhu, Y., Zang, F., Wang, Q., … Xie, C. (2020). Disrupted rich-club network organization and individualized identification of patients with major depressive disorder. Progress in Neuro-Psychopharmacology & Biological Psychiatry, *108*, 110074. https://doi.org/10.1016/j.pnpbp.2020.110074

Margulies, D. S., Ghosh, S. S., Goulas, A., Falkiewicz, M., Huntenburg, J. M., Langs, G., … Smallwood, J. (2016). Situating the default-mode network along a principal gradient of macroscale cortical organization. *Proceedings of the National Academy of Sciences*, *113*(44), 12574–12579. https://doi.org/10.1073/pnas.1608282113

Mulders, P. C., van Eijndhoven, P. F., Schene, A. H., Beckmann, C. F., & Tendolkar, I. (2015). Resting-state functional connectivity in major depressive disorder: A review. *Neuroscience & Biobehavioral Reviews*, *56*, 330–344. https://doi.org/10.1016/j.neubiorev.2015.07.014

Nabulsi, L., McPhilemy, G., Kilmartin, L., Whittaker, J. R., Martyn, F. M., Hallahan, B., … Cannon, D. M. (2020). Frontolimbic, frontoparietal, and default mode involvement in functional dysconnectivity in psychotic bipolar disorder. *Biological Psychiatry: Cognitive Neuroscience and Neuroimaging*, *5*(2), 140–151. https://doi.org/10.1016/j.bpsc.2019.10.015

Nixon, N. L., Liddle, P. F., Nixon, E., Worwood, G., Liotti, M., & Palaniyappan, L. (2014). Biological vulnerability to depression: Linked structural and functional brain network findings. *British Journal of Psychiatry*, *204*, 283–289. https://doi.org/10.1192/bjp.bp.113.129965

Osmanlioglu, Y., Tunc, B., Parker, D., Elliott, M. A., Baum, G. L., Ciric, R., … Verma, R. (2019). System-level matching of structural and functional connectomes in the human brain. *NeuroImage*, *199*, 93–104. https://doi.org/10.1016/j.neuroimage.2019.05.064

Paquola, C., Vos De Wael, R., Wagstyl, K., Bethlehem, R. A. I., Hong, S. J., Seidlitz, J., … Bernhardt, B. C. (2019). Microstructural and functional gradients are increasingly dissociated in transmodal cortices. *PLoS Biology*, *17*(5), e3000284. https://doi.org/10.1371/journal.pbio.3000284

Preti, M. G., & Van De Ville, D. (2019). Decoupling of brain function from structure reveals regional behavioral specialization in humans. *Nature Communications*, *10*(1), 4747. doi:10.1038/s41467-019-12765-7

Qin, P., Liu, Y., Shi, J., Wang, Y., Duncan, N., Gong, Q., … Northoff, G. (2012). Dissociation between anterior and posterior cortical regions during self-specificity and familiarity: A combined fMRI-meta-analytic study. *Human Brain Mapping*, *33*(1), 154–164. doi:10.1002/hbm.21201

Reinder, V., Larivière, S., Caldairou, B., Hong, S. J., Margulies, D. S., Jefferies, E., … Bernhardt, B. C. (2018). Anatomical and microstructural determinants of hippocampal subfield functional connectome embedding. *Proceedings of the National Academy of Sciences*, *115*(40), 10154–10159.

Rush, A. J., Warden, D., Wisniewski, S. R., Fava, M., Trivedi, M. H., Gaynes, B. N., & Nierenberg, A. A. (2009). STAR*D: Revising conventional wisdom. *CNS Drugs*, *23*(8), 627–647. doi:10.2165/00023210-200923080-00001

Schaefer, A., Kong, R., Gordon, E. M., Laumann, T. O., Zuo, X. N., Holmes, A. J., … Yeo, B. T. T. (2018). Local-global parcellation of the human cerebral cortex from intrinsic functional connectivity MRI. *Cerebral Cortex*, *28*(9), 3095–3114. doi:10.1093/cercor/bhx179

Scheepens, D. S., van Waarde, J. A., Lok, A., de Vries, G., Denys, D., & van Wingen, G. A. (2020). The link between structural and functional brain abnormalities in depression: A systematic review of multimodal neuroimaging studies. *Frontiers in Psychiatry*, *11*, Article 485. https://doi.org/10.3389/fpsyt.2020.00485

Scheinost, D., Holmes, S. E., DellaGioia, N., Schleifer, C., Matuskey, D., Abdallah, C. G., … Esterlis, I. (2018). Multimodal investigation of network level effects using intrinsic functional connectivity, anatomical covariance, and structure-to-function correlations in unmedicated major depressive disorder. *Neuropsychopharmacology*, *43*(5), 1119–1127. https://doi.org/10.1038/npp.2017.229

Shafiei, G., Zeighami, Y., Clark, C. A., Coull, J. T., Nagano-Saito, A., Leyton, M., … Misic, B. (2019). Dopamine signaling modulates the stability and integration of intrinsic brain networks. *Cerebral Cortex*, *29*(1), 397–409. https://doi.org/10.1093/cercor/bhy264

Spati, J., Hänggi, J., Doerig, N., Ernst, J., Sambataro, F., Brakowski, J., … Spinelli, S. (2015). Prefrontal thinning affects functional connectivity and regional homogeneity of the anterior cingulate cortex in depression. *Neuropsychopharmacology*, *40*(7), 1640–1648. https://doi.org/10.1038/npp.2015.8

https://doi.org/10.1017/S0033291724000801 Published online by Cambridge University Press

Suarez, L. E., Markello, R. D., Betzel, R. F., & Misic, B. (2020). Linking structure and function in macroscale brain networks. *Trends in Cognitive Sciences*, *24*(4), 302–315. https://doi.org/10.1016/j.tics.2020.01.008

Thase, M. E., Friedman, E. S., Biggs, M. M., Wisniewski, S. R., Trivedi, M. H., Luther, J. F., … Rush, A. J. (2007). Cognitive therapy versus medication in augmentation and switch strategies as second-step treatments: A STAR*D report. *American Journal of Psychiatry*, *164*(5), 739–752. https://doi.org/10.1176/ajp.2007.164.5.739

Tian, Z., Yamanaka, M., Bernabucci, M., Zhao, M. G., & Zhuo, M. (2017). Characterization of serotonin-induced inhibition of excitatory synaptic transmission in the anterior cingulate cortex. *Molecular Brain*, *10*(1), Article 21. https://doi.org/10.1186/s13041-017-0303-1

Tozzi, L., Goldstein-Piekarski, A. N., Korgaonkar, M. S., & Williams, L. M. (2020). Connectivity of the cognitive control network during response inhibition as a predictive and response biomarker in major depression: Evidence from a randomized clinical trial. *Biological Psychiatry*, *87*(5), 462–472. https://doi.org/10.1016/j.biopsych.2019.08.005

Tzourio-Mazoyer, N., Landeau, B., Papathanassiou, D., Crivello, F., Etard, O., Delcroix, N., … Joliot, M. (2002). Automated anatomical labeling of activations in SPM using a macroscopic anatomical parcellation of the MNI MRI single-subject brain. *NeuroImage*, *15*(1), 273–289. https://doi.org/10.1006/nimg.2001.0978

van den Heuvel, M. P., Sporns, O., Collin, G., Scheewe, T., Mandl, R. C., Cahn, W., … Kahn, R. S. (2013). Abnormal rich club organization and functional brain dynamics in schizophrenia. *JAMA Psychiatry*, *70*(8), 783–792. https://doi.org/10.1001/jamapsychiatry.2013.1328

Van Essen, D. C., Smith, S. M., Barch, D. M., Behrens, T. E., Yacoub, E., Ugurbil, K., & Consortium, W. U.-M. H. (2013). The WU-Minn human connectome project: An overview. *NeuroImage*, *80*, 62–79. https://doi.org/10.1016/j.neuroimage.2013.05.041

Vazquez-Rodriguez, B., Suarez, L. E., Markello, R. D., Shafiei, G., Paquola, C., Hagmann, P., … Misic, B. (2019). Gradients of structure-function tethering across neocortex. *Proceedings of the National Academy of Sciences*, *116*(42), 21219–21227. https://doi.org/10.1073/pnas.1903403116

Vos de Wael, R., Benkarim, O., Paquola, C., Lariviere, S., Royer, J., Tavakol, S., … Bernhardt, B. C. (2020). BrainSpace: A toolbox for the analysis of macroscale gradients in neuroimaging and connectomics datasets. *Communications Biology*, *3*(1), Article 103. https://doi.org/10.1038/s42003-020-0794-7

Whitfield-Gabrieli, S., Moran, J. M., Nieto-Castanon, A., Triantafyllou, C., Saxe, R., & Gabrieli, J. D. (2011). Associations and dissociations between default and self-reference networks in the human brain. *NeuroImage*, *55*(1), 225–232. https://doi.org/10.1016/j.neuroimage.2010.11.048

Yeo, B. T., Krienen, F. M., Eickhoff, S. B., Yaakub, S. N., Fox, P. T., Buckner, R. L., … Chee, M. W. (2016). Functional specialization and flexibility in human association cortex. *Cerebral Cortex*, *26*(1), 465. https://doi.org/10.1093/cercor/bhv260

Zhang, J., Zhang, Y., Wang, L., Sang, L., Yang, J., Yan, R., … Qiu, M. (2017). Disrupted structural and functional connectivity networks in ischemic stroke patients. *Neuroscience*, *364*, 212–225. https://doi.org/10.1016/j.neuroscience.2017.09.009

Zhang, Z., Liao, W., Chen, H., Mantini, D., Ding, J. R., Xu, Q., … Lu, G. (2011). Altered functional-structural coupling of large-scale brain networks in idiopathic generalized epilepsy. *Brain*, *134*(Pt 10), 2912–2928. https://doi.org/10.1093/brain/awr223

Zhao, Y., Zhang, F., Zhang, W., Chen, L., Chen, Z., Lui, S., & Gong, Q. (2021). Decoupling of gray and white matter functional networks in medication-naive patients with major depressive disorder. *Journal of Magnetic Resonance Imaging*, *53*(3), 742–752. https://doi.org/10.1002/jmri.27392

Zhou, H. X., Chen, X., Shen, Y. Q., Li, L., Chen, N. X., Zhu, Z. C., … Yan, C. G. (2020). Rumination and the default mode network: Meta-analysis of brain imaging studies and implications for depression. *NeuroImage*, *206*, Article 116287. https://doi.org/10.1016/j.neuroimage.2019.116287

https://doi.org/10.1017/S0033291724000801 Published online by Cambridge University Press